# Role for neuronal insulin resistance in neurodegenerative diseases

Markus Schubert*†, Dinesh Gautam*†‡, David Surjo†§, Kojihiko Ueki¶, Stephanie Baudler‖**, Dominic Schubert*, Tatsuya Kondo¶, Jens Alber‖**, Norbert Galldiks**††, Eckehardt Küstermann**††, Saskia Arndt§, Andreas H. Jacobs**††, Wilhelm Krone*, C. Ronald Kahn¶, and Jens C. Brüning*‖**‡‡

‖Institute for Genetics, **Center for Molecular Medicine Cologne, §Institute II for Anatomy, and ††Department of Neurology, University of Cologne, and Max Planck Institute for Neurological Research, D-50931 Cologne, Germany; *Klinik II und Poliklinik für Innere Medizine der Universität zu Köln and Center for Molecular Medicine Cologne, D-50924 Cologne, Germany; and ¶Joslin Diabetes Center, Harvard Medical School, One Joslin Place, Boston, MA 02115

Contributed by C. Ronald Kahn, December 31, 2003

**Impairment of insulin signaling in the brain has been linked to neurodegenerative diseases. To test the hypothesis that neuronal insulin resistance contributes to defects in neuronal function, we have performed a detailed analysis of brain/neuron-specific insulin receptor knockout (NIRKO) mice. We find that NIRKO mice exhibit a complete loss of insulin-mediated activation of phosphatidylinositol 3-kinase and inhibition of neuronal apoptosis. In intact animals, this loss results in markedly reduced phosphorylation of Akt and GSK3$\beta$, leading to substantially increased phosphorylation of the microtubule-associated protein Tau, a hallmark of neurodegenerative diseases. Nevertheless, these animals exhibit no alteration in neuronal proliferation/survival, memory, or basal brain glucose metabolism. Thus, lack of insulin signaling in the brain may lead to changes in Akt and GSK3$\beta$ activity and Tau hyperphosphorylation but must interact with other mechanisms for development of Alzheimer's disease.**

The insulin receptor (IR) and its substrates are widely expressed in the CNS; however, the role of insulin signaling in the brain remains debatable. The highest level of IR expression is found in the hypothalamus, and several physiological studies have suggested a role of neuronal IR in the regulation of food intake and energy homeostasis (1, 2). Recent studies using conditional inactivation of the IR in the CNS, intracerebroventricular application of insulin, IR antisense mRNA, and blocking anti-IR antibodies have established a role for neuronal insulin signaling in these processes *in vivo* (3–5). However, there is still controversy over the role of insulin signaling in the regulation of brain glucose metabolism, learning and memory formation, and the development of neurodegenerative diseases (6, 7).

In primary fetal brain cell cultures, insulin plays a role in the control of metabolism and growth (8), and clinically it has been demonstrated that patients suffering from Alzheimer's and Parkinson's diseases exhibit reduced expression of IR in the brain (9). It also has been shown that learning acutely regulates expression and tyrosine phosphorylation of the IR in the hippocampus of rats (10). Taken together, these findings suggest that insulin exerts pleiotropic effects in neurons, including the regulation of neuronal proliferation, apoptosis, synaptic transmission, neuronal degeneration, and learning. However, it is still debated whether impaired glucose tolerance or type 2 diabetes represents a risk factor for neurodegenerative diseases, and, if so, whether insulin resistance in the brain or other metabolic consequences of the pleiotropic syndrome of insulin resistance may contribute to this phenomenon (11). To investigate the impact of isolated CNS-specific insulin resistance *in vivo*, we have performed a detailed analysis of learning, neuronal survival, and the biochemical processes associated with neurodegeneration in mice with conditional inactivation of the IR gene in the CNS, i.e., brain/neuron-specific IR knockout (NIRKO) mice.

## Methods

**Animals and Genotyping.** NIRKO mice were generated as described (3) and backcrossed onto a C57BL/6J background for five generations. Animals were housed on a 12-h light/dark cycle (0200 on/1400 off) and were fed a standard rodent chow. All animal procedures were performed in accordance with the German Laws for Animal Protection and were approved by the local animal care committee and the Bezirksregierung Köln. Imaging was performed under general anesthesia induced by i.p. administration of ketamine/xylazine (120 $\mu$l of 20 mg/ml ketamine/0.4% xylazine in saline per animal).

**Histology and Immunostaining.** For immunostaining, animals were transcardially perfused with PBS followed by perfusion with 4% paraformaldehyde for 30 min. Brains were either paraffin-embedded or cryoprotected in 30% sucrose, and five 30-$\mu$m sections were prepared. Terminal deoxynucleotidyltransferase-mediated dUTP nick end labeling (TUNEL) assays were performed with the DNA FragEL Kit (Oncogene Research Products). Nissl and hematoxylin/eosin staining as well as immunostaining with anti-glial fibrillary acidic protein (GP-52; Progen, Heidelberg) or anti-BrdUrd (Boehringer Mannheim) antibodies was carried out according to the manufacturer's guidelines. Antibodies against phosphatidylinositol-3, 4, 5 phosphate ($PIP_3$) were from Echelon Science (Salt Lake City).

**BrdUrd Incorporation.** BrdUrd (Boehringer Mannheim) at 100 $\mu$g/g of body weight was injected i.p. into mice at postnatal day 6. Tissues were harvested after 6 h, fixed in 4% paraformaldehyde, and processed for immunohistochemistry as described above.

**Isolation and Culture of Cerebellar Granule Cells and Analysis of Neuronal Apoptosis.** Cerebellar granule neurons were isolated and analyzed for neuronal apoptosis by using Hoechst dye 33342.

**Immunoblotting.** Brains or primary cerebellar granule cells were lysed and processed for Western blot analysis as described (3). Primary antibodies against the IR $\beta$-subunit, insulin-like growth factor (IGF)-IR $\beta$-subunit, and Tau (Santa Cruz Biotechnology); Akt, pAkt, glycogen synthase kinase (GSK)3$\beta$, and pGSK3$\beta$ (Upstate Biotechnology, Lake Placid, NY); and AT8 and AT180 (Innogenetic, Ghent, Belgium) were used.

**Morris Water Maze Task.** Animals performed four trials during five daily acquisition sessions plus one session in the next week. Each

Abbreviations: IR, insulin receptor; NIRKO, brain/neuron-specific IR knockout; $PIP_3$, phosphatidylinositol-3, 4, 5 phosphate; IGF, insulin-like growth factor; PET, positron-emission tomography; [$^{18}$F]FDG, 2-[$^{18}$F]fluoro-2-deoxy-D-glucose; ROI, regions of interest; IRS, IR substrates; GSK, glycogen synthase kinase.

†M.S., D.G., and D.S. contributed equally to this work.

‡Present address: National Institutes of Health, Bethesda, MD 20892.

‡‡To whom correspondence should be addressed at: Institut für Genetik der Universität zu Köln, Weyertal 121, D-50931 Cologne, Germany. E-mail: jens.bruening@uni-koeln.de.





www.pnas.org/cgi/doi/10.1073/pnas.0308724101

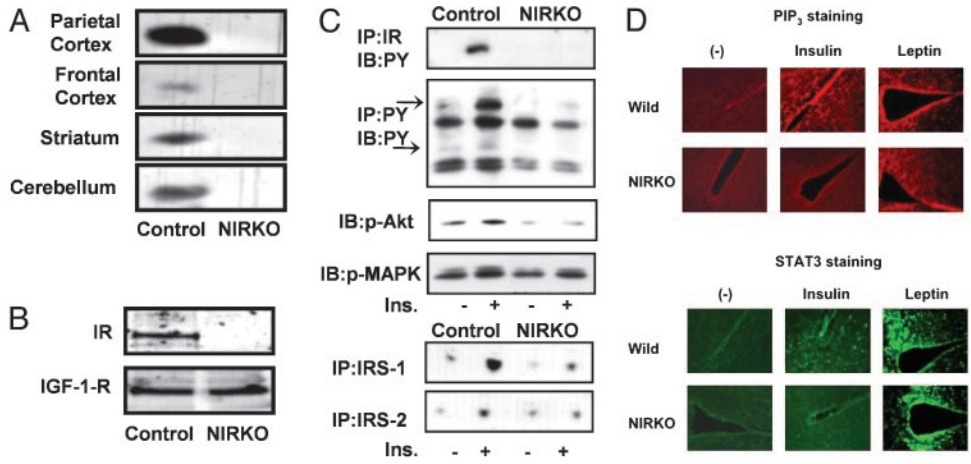


**Fig. 1.** Abolished IR expression and insulin-stimulated signaling in NIRKO neurons. (*A*) Immunoblot analysis of IR expression on protein extracts from microdissected individual brain regions of control and NIRKO mice. (*B*) IR and IGF-1-IR expression in cultured neurons from control and NIRKO mice analyzed by Western blot. The blots were probed with a polyclonal antiserum specific for the $\beta$-subunit of the IGF-IR and the $\beta$-subunit IR. (*C*) Immunoblot analysis of insulin-stimulated tyrosine phosphorylation of the IR $\beta$-subunit (top blot) and of cellular proteins (second blot) on protein extracts from control and NIRKO mice. Insulin-stimulated activation of Akt and Erk by Western blot analysis using phospho-specific antibodies against Akt (Ser-473) and Erk (Tyr-204) from control and NIRKO hypothalami (third and fourth blots) also are shown. Insulin-stimulated IRS-1- and IRS-2-associated phosphatidylinositol 3-kinase activity from control and NIRKO hypothalami (fifth and sixth blots) was determined 15 min after i.v. injection of 5 milliunits of insulin. (*D*) Immunohistochemistry with anti-$PIP_3$ (*Upper*) and anti-pSTAT3 (*Lower*) antibodies. Sections through the hypothalamus were prepared from control (Wild) or NIRKO mice that had been injected with vehicle alone, 5 milliunits of insulin, or 10 $\mu$g of leptin per g of body weight through the tail vein at 30 min before harvesting.

of four starting positions (north, east, south, and west) was used once in a series of four trials in randomized order. A trial was terminated as soon as the mouse had climbed onto the escape platform or when 60 sec had elapsed.

**Open Field (OF) Test.** The OF was a polypropylene box (40 × 40 × 45 cm) with a floor subdivided into 10 × 10-cm squares by lines. A video camera mounted above the OF registered the horizontal movements of the animals. Testing was performed between 0800 and 1200 hours in a quiet room. Immediately after a mouse was placed in the center of the OF, its movements were scored by means of the automatic video-tracking system ETHOVISON (version 1.92; Nodus, Wageningen, The Netherlands) for 5 min on each of 5 successive days.

**Positron-Emission Tomography (PET).** *In vivo* PET imaging was performed in NIRKO mice ($n = 7$) in comparison with wild-type mice ($n = 7$) and was repeated once. Radiolabeled 2-[$^{18}$F]fluoro-2-deoxy-D-glucose ([$^{18}$F]FDG) was administered i.v. (into the tail vein) into experimental animals with doses ranging between 3.7 and 7.4 MBq per mouse. To study [$^{18}$F]FDG tracer accumulation within the brain, PET imaging was performed by using a high-resolution microPET (Concorde Microsystems, Knoxville, TN; 63 image planes; 2.0-mm full width at half maximum). Emission scans (30-min duration) were obtained starting 30–60 min after tracer application. For quantitation of images, a set of [$^{18}$F]FDG reference standards of different radioactivity concentrations was placed within the field of view of the PET scanner. Data evaluation was based on a regions-of-interest (ROI) (1) analysis of transaxial [$^{18}$F]FDG-PET images through brain and mediastinum to determine radioactivity concentrations. Data were corrected for decay and divided by the total injected dose to represent percentage injected dose per gram (%ID/g) and were expressed as the fold difference from background (mediastinum) activity (brain-to-background ratio, B/BG). To ensure proper ROI placement within the brain and to avoid partial volume artifacts from harderian glands (12), [$^{18}$F]FDG-PET images were aligned with high-resolution magnetic resonance images.

**MRI.** *In vivo* MRI was performed with one representative animal per group on a 7-T horizontal animal scanner (BioSpec 70/30; Bruker Biospin, Ettlingen, Germany) equipped with actively shielded gradient coils (200 mT/m) and home-built rf electronics for the optimization of sensitivity. rf pulses were applied by a 12-cm-diameter Helmholtz coil actively decoupled from the single-loop receiver surface coil of 22 mm in diameter. Gradient-echo magnetic resonance images were recorded as 3D data sets with time to repeat/time to echo (TR/TE) = 60/22 ms, excitation pulses of 20°, and a field of view of 30 × 17 × 17 mm, resulting in a pixel resolution of 59 × 132 × 132 $\mu$m. The total measurement time was 17 min.

**Statistical Analysis.** In the Morris water maze task the effect of the mutation in the acquisition of the water escape task was assessed by using ANOVA with the factor mutation (wild-type vs. mutant) and the repeated-measures factor sessions (days 1 to 6 of training) (SAS 8.02 for WINDOWS, SAS Institute, Cary, NC). To compare glucose metabolism in wild-type vs. NIRKO mice, regional values for percentage injected dose per gram (%ID/g) and brain-to-background ratios (B/BG) were compared between both groups by using Student's *t* test (SIGMASTAT 7.0 for WINDOWS, SPSS, Chicago).

## Results

Previously we have shown (3) that mice homozygous for a loxP-flanked exon 4 of the IR gene and expressing Cre-recombinase under control of the rat nestin promoter exhibit a neural tissue-specific knockout of the IR (NIRKO) with >95% reduction in expression of the IR in the brain compared with control mice. In the present study, a similar reduction was observed when several isolated brain regions were analyzed by Western blotting, including frontal and parietal cortices, hippocampus, and cerebellum (Fig. 1*A*). Moreover, analysis of protein extracts from cultured cerebellar granule neurons of NIRKO and control mice revealed that IR expression in NIRKO mice was abolished (Fig. 1*B*). Expression of the IGF-1 receptor, on the other hand, remained unaltered (Fig. 1*B*).

To assess the impact of IR deletion on insulin-stimulated signaling in the brains of NIRKO mice, we analyzed tyrosine

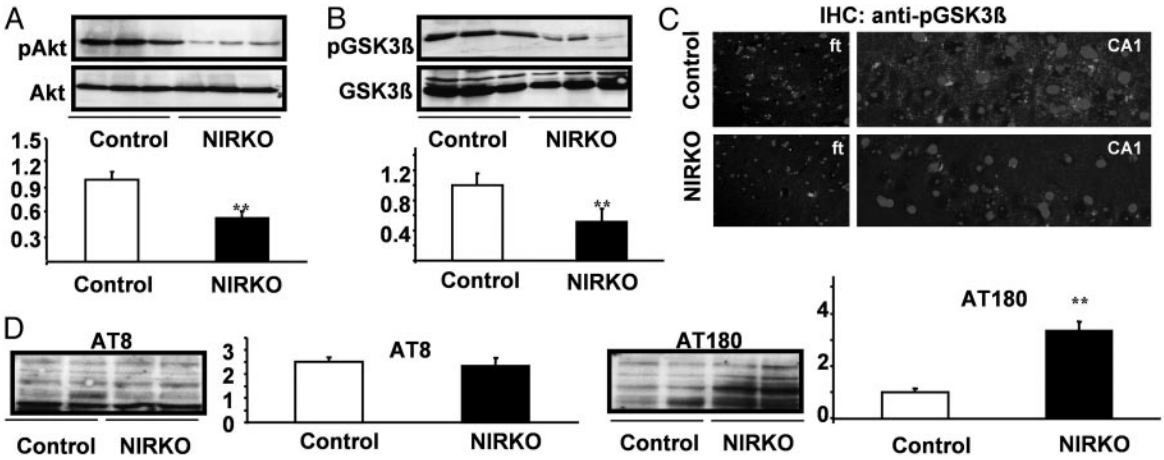


**Fig. 2.** Neuronal insulin resistance causes Tau hyperphosphorylation *in vivo*. (*A*) Western blot analysis of brain extracts derived from individual randomly fed mice with antibodies against Akt or pAkt (Ser-473). (*Lower*) The densitometric quantification as mean ± SEM [control (open bars) and NIRKO (filled bars) mice] of at least eight animals of each genotype is shown (**, $P < 0.01$ by unpaired Student's *t* test). (*B*) Western blot analysis of brain extracts derived from individual randomly fed mice with antibodies against GSK3$\beta$ or pGSK3$\beta$ (Ser-9). (*Lower*) The densitometric quantification as mean ± SEM [control (open bars) and NIRKO (filled bars) mice] of at least eight animals of each genotype (**, $P < 0.01$ by unpaired Student's *t* test). (*C*) Immunohistochemistry of layer V of the frontal cortex (*Left*) and the pyramidal cells of the CA1 region of the hippocampus (*Right*) with antiserum specific for pGSK3$\beta$ (4′,6-diamidino-2-phenylindole counterstaining). (*D*) Immunoblotting of protein extracts from whole brain lysates of control and NIRKO mice with the AT180 (paired helical filament-Tau phosphorylated at Thr-231) and AT8 (paired helical filament-Tau phosphorylated at Ser-202) antibodies. Data represent mean ± SEM [control (open bars) and NIRKO (filled bars) mice] of at least six animals of each genotype (**, $P < 0.01$ unpaired Student's *t* test).

phosphorylation of the IR and other cellular proteins by Western blotting after *in vivo* insulin stimulation. Within 10 min after peripheral i.v. injection, there was a robust stimulation of tyrosine phosphorylation of the IR $\beta$-subunit and the IR substrates (IRS proteins) (Fig. 1*C*). In brain extracts from NIRKO mice, insulin-stimulated tyrosine phosphorylation of the IR and IRS proteins was abolished (Fig. 1*C*). Similarly, insulin almost completely failed to stimulate IRS-1- and IRS-2-associated phosphatidylinositol 3-kinase activity as well as Akt and Erk phosphorylation in brains from NIRKO mice (Fig. 1*C*). These data were substantiated further by the analysis of insulin-stimulated formation of $PIP_3$ by using immunohistochemical staining of $PIP_3$ in hypothalamus. Although insulin potently stimulated $PIP_3$ formation in paraventricular areas and hypothalami of control mice, it failed to do so in NIRKO mice (Fig. 1*D*). Similarly, whereas insulin promoted tyrosine phosphorylation of Stat3 in hypothalami of control mice, it failed to stimulate Stat3 activation in NIRKO mice (Fig. 1*D*). This result was not caused by general inhibition of $PIP_3$ formation and Stat activation, because leptin efficiently stimulated these signaling pathways in NIRKO mice (Fig. 1*D*). These analyses indicate that IR deletion was complete in neurons of NIRKO mice and that insulin-stimulated signaling was abolished without compensatory up-regulation of IGF-1 receptor expression.

Because insulin shares a variety of intracellular signaling components with other growth and neurotrophic factors, we next determined the activation of the $PIP_3$ downstream target Akt, which has been implicated in the regulation of neuronal apoptosis, by Western blot analysis using an antibody that recognizes Akt only when phosphorylated at Ser-473, i.e., in its active state (13). This analysis revealed a >50% reduction of Akt phosphorylation in brain extracts from NIRKO mice as compared with control animals, whereas expression of Akt at the protein level remained unaltered (Fig. 2*A*).

Another downstream target of growth and neurotrophic factor-activated $PIP_3$ signaling is GSK3$\beta$. Consistent with the decrease in Akt phosphorylation, GSK3$\beta$ phosphorylation also was markedly reduced in brain extracts from NIRKO mice as compared with controls, whereas expression of the enzyme remained unaltered (Fig. 2*B*). Immunohistochemical analysis of phosphorylated GSK3$\beta$ also revealed that both the number of cells exhibiting GSK3$\beta$ immunoreactivity and the intensity of signal in labeled cells were reduced in NIRKO brains as compared with controls (Fig. 2*C*).

Phosphorylation of GSK3$\beta$ results in a decrease in enzyme activity (14), and reduced phosphorylation would therefore be expected to result in an increase in activity. In both cultured neurons and transgenic mice, overexpression of active GSK3$\beta$ has been demonstrated to result in increased Tau phosphorylation (15). The microtubule-associated protein Tau physiologically stabilizes microtubules and under pathological conditions is the major component of neurofibrillary tangles detected in neurodegenerative diseases (16). Western blot analysis using the AT180 antibody, which detects Tau phosphorylation at the potential GSK3$\beta$ site Thr-231, revealed a 3.5-fold increase in brains of NIRKO mice (Fig. 2*D*). Interestingly, similar experiments with the antibody AT8, which recognizes Tau phosphorylated at position Ser-202, demonstrated unaltered phosphorylation of this residue in brains of NIRKO mice (Fig. 2*D*). Taken together, these data indicate that neuronal insulin resistance results in reduction of phosphorylation of Akt and GSK3$\beta$ and a 3.5-fold increase of Tau phosphorylation at residue Thr-231. Nevertheless, neurofibrillary tangle formation was not detectable in NIRKO mice up to an age of 18 months (data not shown).

Phosphorylation and activation of Akt has been demonstrated to be essential for the inhibition of neuronal apoptosis (13). Potassium withdrawal resulted in profound induction of apoptosis (≈80%) in cultured cerebellar granule neurons from NIRKO and control mice. In neuronal cells from control mice, this result could largely be prevented by 100 nM IGF-1 and, to a lesser extent, insulin (Fig. 3*A*). These effects were concentration-dependent, with a decrease from 77% apoptotic cells in the absence of insulin/IGF-1 to 50% at a concentration of 10 nM and 35% at 100 nM insulin (Fig. 3*B*). In control cells, IGF-1 was clearly more potent in inhibiting apoptosis than insulin, reducing the percentage of apoptotic cells to ≈15% at a concentration of 100 nM (Fig. 3*C*). By contrast, in neurons cultured from NIRKO mice, insulin almost completely failed to inhibit apoptosis at any concentration (Fig. 3 *A* and *B*). Interestingly, neurons cultured from NIRKO mice also exhibited a shift in the dose–response to

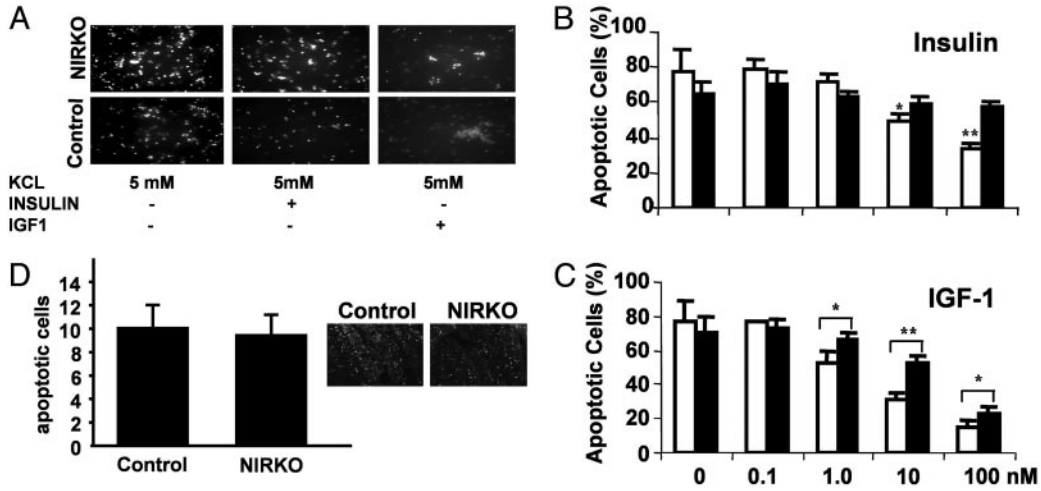


**Fig. 3.** IR expression is required for insulin-stimulated inhibition of apoptosis in cultured neurons but not in the intact animal. (*A*) Cultured cerebellar granule cells of 6-day-old NIRKO (*Upper*) and control (*Lower*) mice were subjected to low KCl-containing (5 mM) medium to induce apoptosis (*Left*); cells were incubated with 100 nM insulin (*Center*) and with 100 nM IGF-1 (*Right*). Condensed nuclei were visualized by Hoechst dye 33342. (*B*) After reduction of KCl concentrations, cells were stimulated with 0, 0.1, 1.0, 10, and 100 nM insulin; control (open bars) and NIRKO (filled bars) mice. Data represent the mean ± SEM of at least eight animals of each genotype. (*C*) Antiapoptotic effect of IGF-1 on primary cerebellar granule cells. After reduction of KCl concentrations, cells were stimulated with 0, 0.1, 1.0, 10, and 100 nM IGF-1; control (open bars) and NIRKO mice (filled bars). Data represent the mean ± SEM of at least eight animals of each genotype. (*D*) Terminal deoxynucleotidyltransferase-mediated dUTP nick end labeling (TUNEL) assays of cerebella from postnatal-day-5 pups of NIRKO mice and their littermate controls. Quantification of apoptotic nuclei in the outer granule layer. Data represent the mean ± SEM of at least four animals of each genotype. (Magnification, ×40.)

the antiapoptotic effect of IGF-1 as compared with cells from control mice ($ED_{50}$ = 7.5 nM IGF-1 for NIRKO cells vs. 2.5 nM for controls). Taken together, these data indicate that, in cultured neurons, insulin mediates its antiapoptotic effect through the IR, and also that IGF-1-induced inhibition of apoptosis also is mediated partly through the IR. Despite the lack of insulin's ability to inhibit apoptosis in cultured neurons, the assessment of apoptotic cells in the intact animals did not reveal any significant differences between control and NIRKO mice (Fig. 3*D*). Furthermore, assessment of neuronal DNA synthesis *in vivo* revealed no difference in the number of BrdUrd-positive cells between NIRKO and control cerebella (data not shown).

Because previous studies have suggested a role for neuronal insulin signaling in cognitive functions under physiological and pathological conditions, we assessed learning and memory formation in NIRKO and control mice by using the Morris water maze at 7 weeks of age. Both control and NIRKO mice progressively reduced the time needed to escape to the hidden platform in repeated test sessions with no significant difference between control and NIRKO mice with respect to the escape latency or the distance moved to reach the platform (Fig. 4*A*). Moreover, motoric performance of NIRKO mice was similar to that of control animals as assessed by swimming speed. Further assessment of motor coordination by performance in the vertical pole test, the upside-down grid, placing response, the rota rod, and grip strength confirmed unaltered motor coordination of NIRKO mice (data not shown). To exclude the possibility that impaired learning as a consequence of neuronal insulin resistance might occur as an age-dependent phenomenon, we repeated the experiments in animals at the age of 40 to 44 weeks. Two different subgroups of mice were studied: mice tested at the age of 7 weeks (experienced group) and mice that had never encountered the Morris water maze task (naive group). The performance of naive, older mice was comparable with that seen in 2-month-old animals with no significant difference between control and NIRKO mice, both with respect to the escape latency (Fig. 4*B*) and the distance moved to reach the platform (data not shown). Direct comparison of the tests over the 9-month interval revealed that, on the second day of the retest, mice of the experienced group exhibited escape latencies and distances moved to reach the platform comparable with those of the last day of the first test (Fig. 4*B*). This long-term memory effect was not different between control and NIRKO mice (Fig. 4*B*). NIRKO mice also performed normally in the open field and T-maze tests, confirming unaltered learning in NIRKO mice and indicating that anxiety-like behavior is unaltered in these animals (data not shown). Taken together, these data indicate that, despite the presence of severe neuronal insulin resistance and increased Tau phosphorylation, NIRKO mice were able to perform normally with respect to spatial learning and memory, both short- and long-term, independent of age.

Because previous work has led to the speculation that neuronal IRs might regulate glucose metabolism in the CNS and because patients with Alzheimer's disease show a characteristic pattern of altered cerebral glucose metabolism, we assessed steady-state cerebral glucose metabolism by microPET *in vivo* (Fig. 4*C*). To ensure proper ROI placement within the brain, [$^{18}$F]FDG-microPET images were coregistered with high-resolution magnetic resonance images (Fig. 4*C*). The [$^{18}$F]FDG brain-to-background ratios (B/BG) were not significantly different between NIRKO and control mice under basal conditions (2.2 ± 0.5 vs. 2.1 ± 0.4; $P$ = not significant). These data indicate that within the limits of this test, basal cerebral glucose metabolism in NIRKO mice was not affected by the lack of neuronal IRs.

## Discussion

NIRKO mice represent a unique model in which to study the consequences of isolated CNS-specific disruption of IR signaling on the biochemistry and function of the brain. The reduced phosphorylation of Akt and GSK3$\beta$ in brains of NIRKO mice, in the presence of otherwise intact neurotrophic signaling, demonstrates directly the relative contribution and importance of IR signaling for the activation of this pathway in the CNS. Moreover, protein extracts from brains of NIRKO mice display a 3.5-fold increase in Tau phosphorylation. Tau is a neuronal

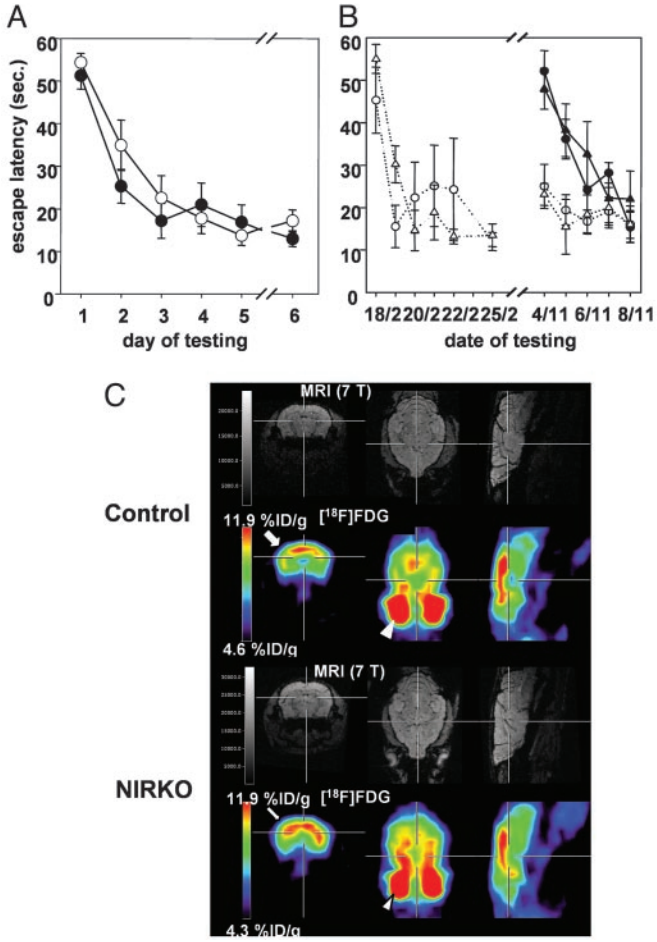


**Fig. 4.** Unaltered spatial learning, long-term memory, and brain glucose metabolism in NIRKO mice. (*A*) Escape latency to find the platform after exposure to the water maze for 7-week-old control (open circles) and NIRKO (filled circles) mice. Data presented per session represent the mean of four trials per session and the mean of seven animals of each genotype ± SEM. (*B*) Escape latency to find the platform after exposure to the water maze for 11-month-old control (circles) and NIRKO (triangles) mice. Data are separated for mice having performed a Morris water maze task at the age of 7 weeks (experienced mice, open symbols) and those that have not before encountered a Morris water maze task (naive mice, filled symbols). Data presented per session represent the mean of four trials per session and the mean of four to seven animals of each genotype ± SEM. (*C*) Shown are representative high-resolution magnetic resonance images (*Upper*) and matched [$^{18}$F]FDG-microPET images (*Lower*) through the brain of a representative control mouse (*Upper*) and a representative NIRKO mouse (*Lower*) [transaxial (*Left*), coronal (*Center*), and sagittal (*Right*)]. ROI were placed in a transaxial plane (arrow). Distinction between brain and hypermetabolic harderian glands (arrowhead) is made by coregistration with MRI.

microtubule-associated protein found predominantly in axons, where it promotes tubulin polymerization and stabilizes microtubules (16).

Hyperphosphorylated Tau is a major component of neurofibrillary lesions characteristic of Alzheimer's disease and other brain dysfunctions. Immunoblotting revealed site-specific Tau hyperphosphorylation at Thr-231 but not at Ser-202. Phosphorylation of Tau at Thr-231 in humans has been correlated with cognitive decline and suggested as a biomarker for Alzheimer's disease (17). These findings in NIRKO mice are in contrast to those obtained in mice lacking IRS-2, which also exhibit Tau hyperphosphorylation, but this occurs exclusively at Ser-202 (18), a presumed site of cyclin-dependent kinase phosphorylation (19). Interestingly, IRS-2-deficient mice exhibit increased GSK3$\beta$ phosphorylation and show reduced expression of the scaffold and catalytic subunit of the Tau-phosphatase PP2A (18). On the other hand, expression of PP2A is unaltered in NIRKO mice (data not shown). These data indicate phosphorylation-site-specific alterations of Tau phosphorylation in different models of neuronal insulin resistance and suggest that IRS-2 may regulate PP2A through signals initiated by receptors other than the IR, and that IR recruits substrates other than IRS-2 for regulating GSK3$\beta$ activity in the brain.

Increased Tau phosphorylation resulting from decreased GSK3$\beta$ phosphorylation in NIRKO mice is consistent with *in vivo* findings obtained in mice overexpressing constitutively active GSK3$\beta$ in the CNS (15). These GSK3$\beta$ transgenic mice exhibit Tau hyperphosphorylation at Thr-231 as detected by AT180 but, in contrast to NIRKO mice, also develop deficiencies in cognitive functions, linking increased GSK3$\beta$ activity to neuronal apoptosis and neurodegeneration (15). Whether this is a quantitative or qualitative difference in the GSK3$\beta$ activity is unclear. Analysis of NIRKO mice failed to detect any deficiencies in learning and memory; however, the level of GSK3$\beta$ activation in these mice is less than that resulting from transgenic overexpression of a mutant enzyme. Our findings are consistent with the data indicating that insulin resistance might predispose for development of the disease and that insulin resistance alone is not sufficient for the development of overt neurodegenerative changes. Indeed, none of the animal models for Alzheimer's disease resulting from a single genetic manipulation resembles the full clinical phenotype of this disease (20, 21). Therefore, future experiments will have to address the impact of neuronal insulin resistance on the development of neurodegenerative diseases in the context of other mouse models for Alzheimer's disease, such as mice overexpressing mutant APP or presenilin.

Our study also shows that the IR mediates insulin's antiapoptotic effect in neurons. These data confirm the fact that insulin is capable of inhibiting apoptosis in cerebellar granule cells (8) and demonstrate that this response is completely dependent on the presence of the IR rather than on the IGF receptor. Interestingly, IGF-1's ability to inhibit apoptosis also was impaired in neurons cultured from NIRKO mice. This phenomenon could be explained by at least two mechanisms. First, IGF-1 also binds to and activates IRs, and maximum IGF-1-stimulated signaling thus depends on IRs. Alternatively, IRs and IGF-1 receptors form heterodimers, and this heterodimerization might be necessary for sensitive IGF-1's mediated signaling (22). In contrast to our findings in cultured neurons, brains from NIRKO mice exhibited no alterations in development and structure or evidence of increased apoptosis *in vivo*. Thus, the role of the IR *in vivo* can be compensated for by other neurotrophic factors in NIRKO mice. This finding is particularly striking in the face of the significantly reduced Akt activation but consistent with the apparent lack of an apoptotic phenotype of heterozygous Akt-deficient mice (23).

Attempts to address insulin's effect on learning and memory in animals have so far been limited by the availability of adequate technical approaches. Lannert *et al.* (24) have described the intracerebroventricular injection of streptozotocin in rats as a model for neuronal insulin resistance and inferred from the impaired learning performance of these rats a role for neuronal insulin signaling in memory formation. Clearly, this drug that acts to destroy $\beta$ cells *in vivo* may have effects beyond serving as an inhibitor of neuronal insulin signaling. Our data on normal performance of NIRKO mice in the Morris water maze task are also in contrast to recent reports describing an improvement in memory formation after intranasal application of insulin, which raises specifically insulin concentrations in the spinal fluid (25, 26). This apparent contradiction might be explained by the fact that at high concentrations insulin's central effects could be

mediated through the activation of IGF-1 receptors or that acute effects of insulin are different from those of chronic lack of signaling. In any case, the data in NIRKO mice clearly rule out a role for isolated impairment of neuronal IR signaling in the development of impaired cognitive functions.

Although the brain is classically viewed as an organ metabolizing glucose independent of insulin, there has been growing biochemical evidence for expression of the insulin-sensitive glucose transporter GLUT-4 in the CNS and insulin regulation of GLUT-1 expression in other tissues (27, 28). More recently, it has been demonstrated that the related IGF-1 is required for brain glucose metabolism in mice (29). In humans it has been demonstrated that insulin acutely regulates brain glucose metabolism during euglycemic hyperinsulinemic clamp studies (30), and by using labeled 2-deoxyglucose we have found decreased glucose uptake in brains of NIRKO mice during a euglycemic hyperinsulinemic clamp (S. Fisher, J.C.B., and C.R.K., unpublished data). In the present study, steady-state brain glucose metabolism under basal conditions, as assessed by PET imaging in NIRKO mice *in vivo*, was normal. This finding suggests that neuronal IRs are not required for the regulation of basal brain glucose metabolism. Alternatively, an effect is observed only at higher insulin concentrations, such as those that occur during a clamp, and involves the related IGF-1 receptor or is below the limit of detection by PET scanning.

In summary, neuronal IR-mediated signaling appears to have no effect on neuronal growth, glucose uptake, or apoptosis *in vivo* and is not sufficient to fully mimic the development of Alzheimer's disease. On the other hand, abolishing neuronal insulin signaling in NIRKO mice leads to major alterations in Akt and GSK3$\beta$ phosphorylation and, presumably, activity, and hyperphosphorylation of the Tau protein at sites associated with neurodegenerative disease. These observations provide an *in vivo* molecular mechanism in which altered insulin signaling in the brain leads to one of the hallmarks of Alzheimer's disease and demonstrate how neuronal insulin resistance potentially predisposes for the development of neurodegeneration, creating a clinical link between type 2 diabetes and nonvascular dementia.

We thank G. Schmall for excellent secretarial assistance and H. J. van der Staay for advice regarding mouse behavioral analysis. This study was supported by grants from the Bundesministerium für Bildung, Wissenschaft, Forschung, und Technologie (ZMMK-TV2 to J.C.B. and W.K.), the Deutsche Forschungsgemeinschaft (to J.C.B.), the Volkswagen Stiftung (to J.C.B. and W.K.), the Köln Fortune program (to M.S. and J.C.B.), and the National Institutes of Health (DK 31036 to C.R.K.).

1. Woods, S. C., Lotter, E. C., McKay, L. D. & Porte, D., Jr. (1979) *Nature* **282,** 503–505.
2. Woods, S. C., Porte, D., Jr., Bobbioni, E., Ionescu, E., Sauter, J. F., Rohner-Jeanrenaud, F. & Jeanrenaud, B. (1985) *Am. J. Clin. Nutr.* **42,** 1063–1071.
3. Bruning, J. C., Gautam, D., Burks, D. J., Gillette, J., Schubert, M., Orban, P. C., Klein, R., Krone, W., Muller-Wieland, D. & Kahn, C. R. (2000) *Science* **289,** 2122–2125.
4. Obici, S., Feng, Z., Karkanias, G., Baskin, D. G. & Rossetti, L. (2002) *Nat. Neurosci.* **5,** 566–572.
5. Schwartz, M. W., Woods, S. C., Porte, D., Jr., Seeley, R. J. & Baskin, D. G. (2000) *Nature* **404,** 661–671.
6. Wickelgren, I. (1998) *Science* **280,** 517–519.
7. Gasparini, L., Netzer, W. J., Greengard, P. & Xu, H. (2002) *Trends Pharmacol. Sci.* **23,** 288–293.
8. Tanaka, M., Sawada, M., Yoshida, S., Hanaoka, F. & Marunouchi, T. (1995) *Neurosci. Lett.* **199,** 37–40.
9. Moroo, I., Yamada, T., Makino, H., Tooyama, I., McGeer, P. L., McGeer, E. G. & Hirayama, K. (1994) *Acta Neuropathol.* **87,** 343–348.
10. Zhao, W., Chen, H., Xu, H., Moore, E., Meiri, N., Quon, M. J. & Alkon, D. L. (1999) *J. Biol. Chem.* **274,** 34893–34902.
11. Ott, A., Stolk, R. P., van Harskamp, F., Pols, H. A., Hofman, A. & Breteler, M. M. (1999) *Neurology* **53,** 1937–1942.
12. Fukuyama, H., Hayashi, T., Katsumi, Y., Tsukada, H. & Shibasaki, H. (1998) *Neurosci. Lett.* **255,** 99–102.
13. Dudek, H., Datta, S. R., Franke, T. F., Birnbaum, M. J., Yao, R., Cooper, G. M., Segal, R. A., Kaplan, D. R. & Greenberg, M. E. (1997) *Science* **275,** 661–665.
14. Stambolic, V. & Woodgett, J. R. (1994) *Biochem. J.* **303,** 701–704.
15. Lucas, J. J., Hernandez, F., Gomez-Ramos, P., Moran, M. A., Hen, R. & Avila, J. (2001) *EMBO J.* **20,** 27–39.
16. Himmler, A., Drechsel, D., Kirschner, M. W. & Martin, D. W., Jr. (1989) *Mol. Cell. Biol.* **9,** 1381–1388.
17. Buerger, K., Teipel, S. J., Zinkowski, R., Blennow, K., Arai, H., Engel, R., Hofmann-Kiefer, K., McCulloch, C., Ptok, U., Heun, R., *et al*. (2002) *Neurology* **59,** 627–629.
18. Schubert, M., Brazil, D. P., Burks, D. J., Kushner, J. A., Ye, J., Flint, C. L., Farhang-Fallah, J., Dikkes, P., Warot, X. M., Rio, C., *et al*. (2003) *J. Neurosci.* **23,** 7084–7092.
19. Takahashi, S., Saito, T., Hisanaga, S., Pant, H. C. & Kulkarni, A. B. (2003) *J. Biol. Chem.* **278,** 10506–10515.
20. Janus, C. & Westaway, D. (2001) *Physiol. Behav.* **73,** 873–886.
21. van Leuven, F. (2000) *Prog. Neurobiol.* **61,** 305–312.
22. Treadway, J. L., Frattali, A. L. & Pessin, J. E. (1992) *Biochemistry* **31,** 11801–11805.
23. Chen, W. S., Xu, P. Z., Gottlob, K., Chen, M. L., Sokol, K., Shiyanova, T., Roninson, I., Weng, W., Suzuki, R., Tobe, K., *et al*. (2001) *Genes Dev.* **15,** 2203–2208.
24. Lannert, H. & Hoyer, S. (1998) *Behav. Neurosci.* **112,** 1199–1208.
25. Kern, W., Peters, A., Fruehwald-Schultes, B., Deininger, E., Born, J. & Fehm, H. L. (2001) *Neuroendocrinology* **74,** 270–280.
26. Born, J., Lange, T., Kern, W., McGregor, G. P., Bickel, U. & Fehm, H. L. (2002) *Nat. Neurosci.* **5,** 514–516.
27. El Messari, S., Ait-Ikhlef, A., Ambroise, D. H., Penicaud, L. & Arluison, M. (2002) *J. Chem. Neuroanat.* **24,** 225–242.
28. Sankar, R., Thamotharan, S., Shin, D., Moley, K. H. & Devaskar, S. U. (2002) *Brain Res. Mol. Brain Res.* **107,** 157–165.
29. Cheng, C. M., Reinhardt, R. R., Lee, W. H., Joncas, G., Patel, S. C. & Bondy, C. A. (2000) *Proc. Natl. Acad. Sci. USA* **97,** 10236–10241.
30. Bingham, E. M., Hopkins, D., Smith, D., Pernet, A., Hallett, W., Reed, L., Marsden, P. K. & Amiel, S. A. (2002) *Diabetes* **51,** 3384–3390.